AN ABSTRACT OF THE THESIS OF

SAMUEL SEIJI MATSUO for the M.S. in
(Name) (Degree)

ELECTRICAL ENGINEERING
(Major)

Date thesis is presented August 11, 1965

Title DETERIORATION OF GALLIUM ARSENIDE DIODES

Abstract approved
(Major professor)

Changes in the diode characteristics of three different types of diodes were studied. These were point-contact, bonded and zinc-diffused diodes. The parameters in which measurable changes were observed were the forward resistance, the reverse breakdown voltage, the forward "knee" of the diode curve and the constant of proportionality relating the reverse-bias capacitance to voltage. Of the three diodes tested, the bonded diodes, appeared to be the most stable.

The forward resistance increased with time under load conditions for all types of diodes. In the zinc-diffused diodes large initial changes were observed, similar to those observed by Shibata. (19) The final rates of deterioration for all three diodes were about the same. This suggests that the mechanism of deterioration in this portion of the curves may be the same for all three types of diodes.

For the final portions of the deterioration curves of the diffused diodes, the absolute value of load current is related to changes in resistance by $\Delta R = K \sqrt{t} I$ where K is a constant. Difficulty in determining the actual cross sectional area of the diodes prevented relating these changes to current density.

In the worst case the proportionality constant relating voltage to reverse-bias capacitance varied from $V^{-1/2.3}$ to $V^{-1/3.7}$ for diffused diodes. This indicates that the type of junction changed from a step to a PIN type.

The voltage at the forward "knee" of the diode curve increased for the bonded diodes while it decreased for the point-contact and the diffused diodes. An increase in junction barrier height may be responsible for the variation in the bonded diodes while an increase in surface recombination states may be responsible for the decrease in the point-contact case. The spreading of the pn junction by diffusion of an electrically active element is a possible cause of the change in diffused diodes.

DETERIORATION OF
GALLIUM ARSENIDE DIODES

by

SAMUEL SEIJI MATSUO

A THESIS

submitted to

OREGON STATE UNIVERSITY

in partial fulfillment
of the requirements for the
degree of

MASTER OF SCIENCE

June 1966

APPROVED:

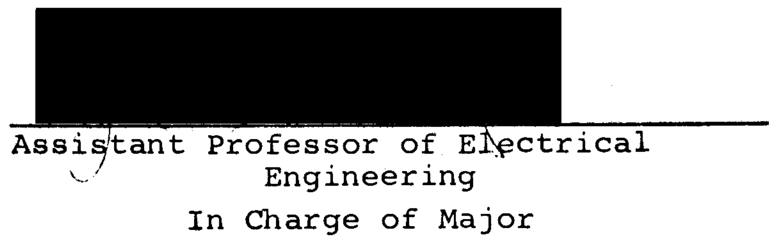

Assistant Professor of Electrical Engineering

In Charge of Major

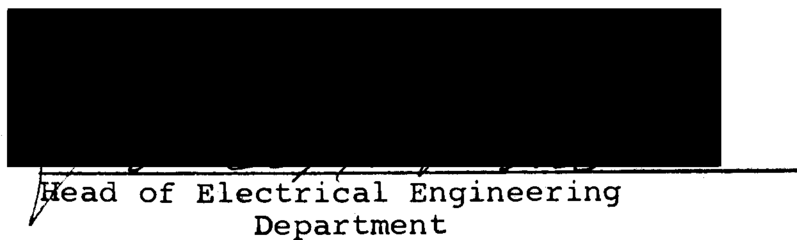

Head of Electrical Engineering Department

Dean of Graduate School

Date thesis is presented August 11, 1965

Typed by Erma McClanathan

ACKNOWLEDGMENTS

The author wishes to express his very sincere and deep appreciation to Professor James C. Looney for his continuous guidance and constructive criticism during the course of this research.

Gratitude is expressed to Tektronix, Inc. for providing the diodes that were used in this work and also to several persons in the Tektronix research laboratory who provided the author with useful technical information.

TABLE OF CONTENTS

	Page
Introduction..................................	1
Theoretical Discussion........................	3
The Planar PN Diode...........................	3
Metal-Semiconductor Contacts..................	9
Experimental..................................	10
Objective.....................................	10
Description of Experimental Samples...........	10
Description of Test Equipment.................	11
Experimental Results..........................	17
Phase I. The Zinc-Diffused Diodes.............	17
Phase II. The Bonded Diodes...................	23
Phase III. The Point-Contact Diodes...........	26
Correlation of the Results....................	30
Discussion of the Results.....................	34
Summary.......................................	39
Bibliography..................................	41
Appendix......................................	43

LIST OF FIGURES

Figure		Page
1.	Charge Distribution in a Planar pn Junction.	3
2.	Small Signal Equivalent Circuit for a Planar pn Junction	5
3.	Physical Construction of a Zinc-Diffused Diode	11
4.	Cases Used to Encapsulate Diodes Used in the Experiment	12
5.	Typical Diode Characteristics	13
6.	Schematic for Circuit Used to Measure Reverse-Bias Capacitance as a Function of Reverse Voltage	14
7.	Schematic for Circuit Used as Constant-Current Power Supply and R_f, V_B and V_f Measuring Device	15
8.	Transient Variations in Forward Resistance (at 10 ma) of Point Contact Diodes Due to Heating	18
9.	Typical Examples of Curves Plotted for Diffused Diodes at 20 ma Load Current	19
10.	Average Change in Resistance for Zinc-Diffused Diodes at Different Load Currents	21
11.	Change in Exponential Proportionality Constant n Relating Voltage to Reverse-Bias Capacitance	22
12.	Changes in V_f for the Three Different Diode Types	24
13.	Forward Resistance Change for Bonded Diodes.	25
14.	Example of a Point Contact Diode Exhibiting Abrupt Change in Forward Resistance	27

Figure | Page

15. Changes in Resistivity of Point-Contact Diodes.......... 28

16. Change in V_B for Point-Contact Diodes...... 29

17. Comparison of Changes in R_f of the Different Diode Types at 20 ma............. 31

18. Comparison of Changes in V_f of the Different Diode Types at 20 ma............. 32

19. Comparison of Changes in V_B of the Different Diode Types at 20 ma............. 33

20. A Plot of $\Delta R/\Delta\sqrt{t}$ as a Function of Load Current for Zinc-Diffused Diodes........... 38

APPENDIX

Table | Page

I Branch Currents under Different Load Conditions with 100 ma Total Current......... 43

II Calibration Errors at Various Calibration Points.......................... 43

DETERIORATION OF GALLIUM ARSENIDE DIODES

INTRODUCTION

Since 1952 there has been increasing interest in the group III - group V compounds as possible competitors of silicon and germanium for use in semiconductor devices. Gallium arsenide, because of its energy gap of 1.37 ev and high electron mobility, has been considered a prime candidate for some applications. However, the electrical characteristics of many gallium arsenide devices change with time under load conditions. It is this property of GaAs that was studied in this experiment.

The mechanisms involved are not well known. Longini (14) has suggested that rapid diffusion of zinc in GaAs caused the changes in zinc-diffused devices. But deterioration has been noted in GaAs devices that are not zinc-diffused. Point-contact GaAs diodes, for example, show changes in characteristics under forward bias. This suggests that possibly an electrically active element other than zinc is responsible for the change.

Many workers in the field have noted that GaAs presents some peculiarities that cannot be explained by laws and equations previously found for germanium and silicon. For instance, the diffusion of zinc vapor into GaAs cannot be described in the customary manner by the diffusion constant of the form $D = D_o \exp(-E/kT)$

where E is the activation energy. (4, 5, 6) Instead the penetration curves show a much steeper front than would be theoretically expected. Goldstein and others (6, 21) have attributed this to zinc diffusing in both the substitutional form and the interstitial form, the rate of penetration of these modes being different by orders of magnitude. In silicon and germanium diffusion takes place in the substitutional mode.

Shibata (19) investigated the deterioration of zinc-diffused tunnel diodes. He forward biased the diodes and found that the peak current of the tunnel diodes decreased constantly as the square root of time. Three distinct slopes were observed. Shibata concluded that thermal effects were not responsible for the changes which he assumed were caused by rapid zinc diffusion under an applied electric field.

In the present study, the deterioration of three different types of GaAs diodes was studied. The zinc-diffused diodes were of special interest since results could be compared with those found by others. The bonded and the point-contact diodes nevertheless were also of great interest since most workers studying the zinc-diffused devices attributed the changes to rapid zinc diffusion. The validity of this assumption has not been proven conclusively.

THEORETICAL DISCUSSION

THE PLANAR PN DIODE

General Description of Diode Action. Classically the planar pn diode is considered to be comprised of three sections, the p-region, the n-region, and the barrier region which is located between the first two. At equilibrium two types of currents exist which exactly cancel each other, being equal in magnitude and opposite in direction. These currents are the diffusion current due to the gradient of holes and electrons that exists between the p- and n-regions and the drift current due to the internal fields in the semiconductor junction. Figure 1 illustrates this idea. The drift

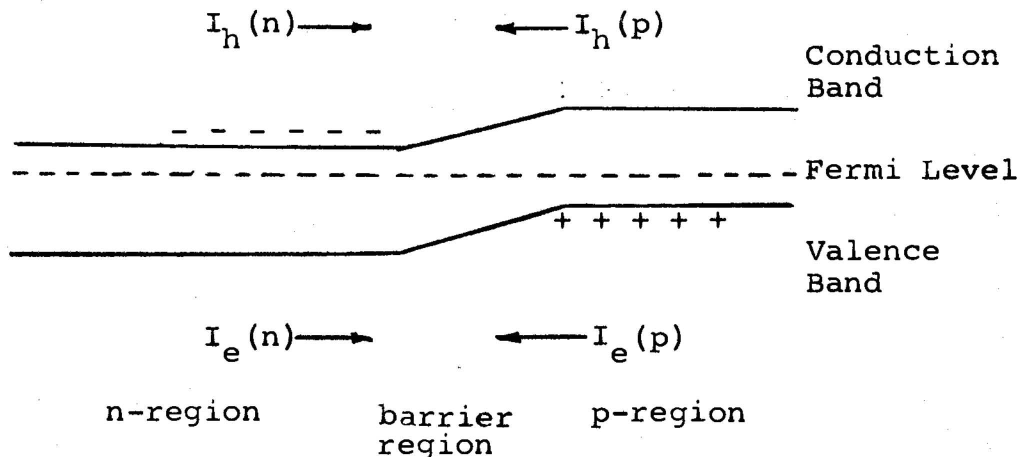

Figure 1. Charge Distribution in a Planar PN Junction.

current due to minority holes in the n-region, $I_h(n)$, is identically equal and opposite in direction to the diffusion current due to holes in the p-region, $I_h(p)$. The same thing holds for electronic currents. (3, p. 191)

At equilibrium there exists an internal electric field directed towards the n-region from the p-region. When the diode is forward biased, that is, when the p-region is made positive compared to the n-region, the external field opposes the internal field. The diffusion current which had been kept small by the high internal barrier now finds less opposition and increases rapidly as the external bias is increased. The drift current is relatively unaffected by the external bias since it primarily depends on the number of thermally generated minority carriers arriving at the junction.

When the diode is reverse biased, the external field aids the internal field. The diffusion current finds increasing opposition to flow and is greatly reduced. The drift current is again unaffected since the arrival of minority carriers at the junction is relatively unaffected by the external bias.

A small signal equivalent circuit is shown in Figure 2. (3) Here C_T is the voltage-dependent barrier capacitance, C_S is the capacitance due to the stored charge in the n- and p-regions, g is the conductance

associated with the rectifying barrier and r_s is the resistance due to the n- and p-regions.

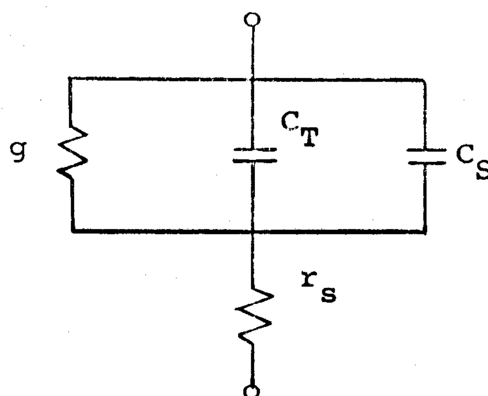

Figure 2. Small Signal Equivalent Circuit for a Planar PN Junction.

The theoretical relation between voltage, V, and current, I, in a pn diode is given by the equation $I = I_s \left[\exp (qV/kT) -1\right]$ where I_s is the saturation current and V and I are taken as positive when the diode is forward biased. For large negative values of V, exp (qV/kT) is much less than 1 and hence $I = -I_s$. For large positive values of V, exp (qV/kT) is much greater than 1 and the current through the diode will depend exponentially on V.

An appreciable portion of the forward current is carried by injected excess current carriers. (8, p. 3-6) If the lifetime of the injected carriers is long, the "shape" of the current-voltage characteristic is

unaffected by the material used and depends only upon temperature. (3, p. 195) The properties of the material enter into the current-voltage equation through the constant I_s, the saturation current.

The conductance of the barrier is given by

$$g = \frac{q}{kT} \quad (I + I_s) \qquad (1.1)$$

At room temperature the constant is about 40 mhos per ampere. (3, p. 196)

The residual resistance or the body resistance of the diode is given by

$$r_s = \frac{l_p}{Ag_p} + \frac{l_n}{Ag_n} \qquad (1.2)$$

where A is the diode cross-sectional area, the l's are the lengths along the current direction of the n and p regions and the g's are the conductivities.

At large reverse bias, g tends toward $\frac{2q}{kT} I_s$ and becomes the dominating resistive factor. For forward biased conditions, however, r_s tends to be the dominating resistive factor.

<u>Capacitive Effects</u>. As pointed out in the diode model shown in Figure 2, there are two types of capacitive reactances to consider. First take the barrier region capacitance C_T. This capacitance is

due to the existence of space-charge layers in the barrier region. These space-charge layers act like capacitive plates and the barrier region between these layers having very few charge carriers acts as a dielectric. Since the width of the barrier region, and hence the distance between the space-charge layers, depends on applied voltage, C_T also depends on the applied voltage, that is,

$$C_T = \frac{EA}{W} \tag{1.3}$$

where W is the distance between the charge layers.

The distance W has been studied with relation to applied external voltage and for step junctions it varies as $V^{\frac{1}{2}}$ and for linearly graded junctions it varies as $V^{1/3}$. Smaller exponential values have been related to PIN type junctions.

When the diode is forward biased, minority carriers swept across the junction form a concentration gradient in the p- and n-regions. If the lifetimes of the minority carriers are long enough, they diffuse for quite a distance before recombining. The uncombined minority carriers represent "stored charge" and at low frequencies appear in circuit equations as a shunting capacitance C_s having the value (3, p. 199)

$$C_s = \tfrac{1}{2} \; (g_p \tau_p + g_n \tau_n) \tag{1.4}$$

where the g's are conductances and τ's are lifetimes of minority holes and electrons.

Reverse-Voltage Breakdown. S. L. Miller (20, p. 206) studied the breakdown voltage for germanium and silicon step pn junctions and found that it was a continuous function increasing as the resistivity of the material increased. The mechanism now associated with this breakdown is that of avalanche breakdown. In this concept holes or electrons are considered to be accelerated so high that on collision more high energy holes and electrons are created. These new particles are in turn of sufficiently high energy to create more holes and electrons so that a multiplicative effect takes place causing the sharp change in characteristics.

Surface Effects. The surface may affect diode characteristics in two important ways. It can shunt the junction by direct surface conductivity or by a high rate of recombination at the surface. If the recombination at the surface is large enough, the reverse characteristics become ohmic because of the large saturation current. The forward characteristics also become ohmic since the injected carriers immediately combine.

METAL-SEMICONDUCTOR CONTACTS

General Description of Diode Action. The general aspects of metal-semiconductor junctions are very similar to pn junctions. The diode current equation is still valid and so is the idea of the small-signal diode model. However, there are some interesting differences.

The barrier in a metal-semiconductor junction arises when electrons from the material with the higher Fermi level flow into the other material. This is necessary since the Fermi level must be the same when the two materials are brought into contact. The shift of electrons which stay close to the junction causes an internal field and hence a barrier.

As pointed out previously, an appreciable fraction of the forward bias current is carried by injected carriers. In the case of point-contact diodes this injection effect lowers the forward resistance quite markedly. This results from the fact that in point contacts, the resistance is concentrated very near the point due to the high current densities there. The injected carriers have maximum effect near the point of injection since the effect is dependent on the diffusion length of the carriers. Hence, in point contacts, the injected carriers affect the forward resistance to a great degree.

EXPERIMENTAL

OBJECTIVE

The purpose of this study was to observe the deterioration of three types of diodes under various current loadings. Of interest were the change in the forward resistance, the reverse breakdown voltage, the reverse bias capacitance and the forward bias "knee" of the diode curve. These parameters have been found to vary with time and a comparison between the changes in the different diodes at different current loadings was made.

DESCRIPTION OF EXPERIMENTAL SAMPLES

Three types of GaAs diodes were used in this experiment. These were the zinc-diffused, the point-contact and the bonded. Figure 3 shows the physical construction of the zinc-diffused diodes. The junction area was about 1 mil in diameter and the depth of diffusion was about 0.3 mils. The p contact was an evaporated gold film and the n contact was an alloy of germanium and gold.

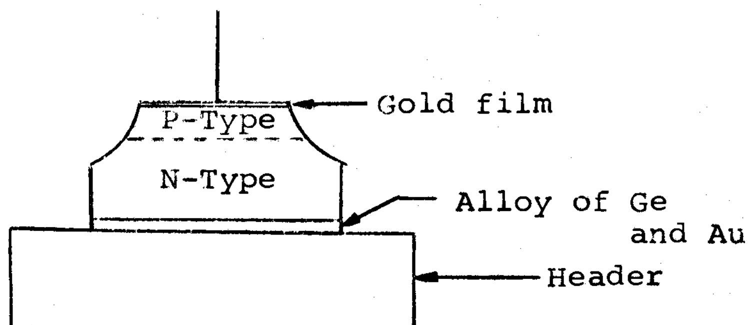

Figure 3. Physical Construction of a Zinc-Diffused Diode.

For the point-contact diode, a whisker of phosphor-bronze was used as the point contact. The reverse side contact was an alloy of nickel and gold. For the bonded diode, an aluminum lead was bonded to one side of the chip. The reverse side was an alloy of germanium and gold.

All diodes were hermetically sealed to minimize surface effects. Figure 4 shows the external view of the different diodes. Typical characteristics of the three types of diodes are presented in Figure 5.

DESCRIPTION OF TEST EQUIPMENT

A schematic diagram for the circuit used to measure reverse-bias capacitance as a function of voltage is given in Figure 6. The placement of the voltmeter as shown measures the voltage across the diode quite accurately for the diffused diodes. The LC-meter has a

Best scan available. Orginal is a photocopy of a copy.

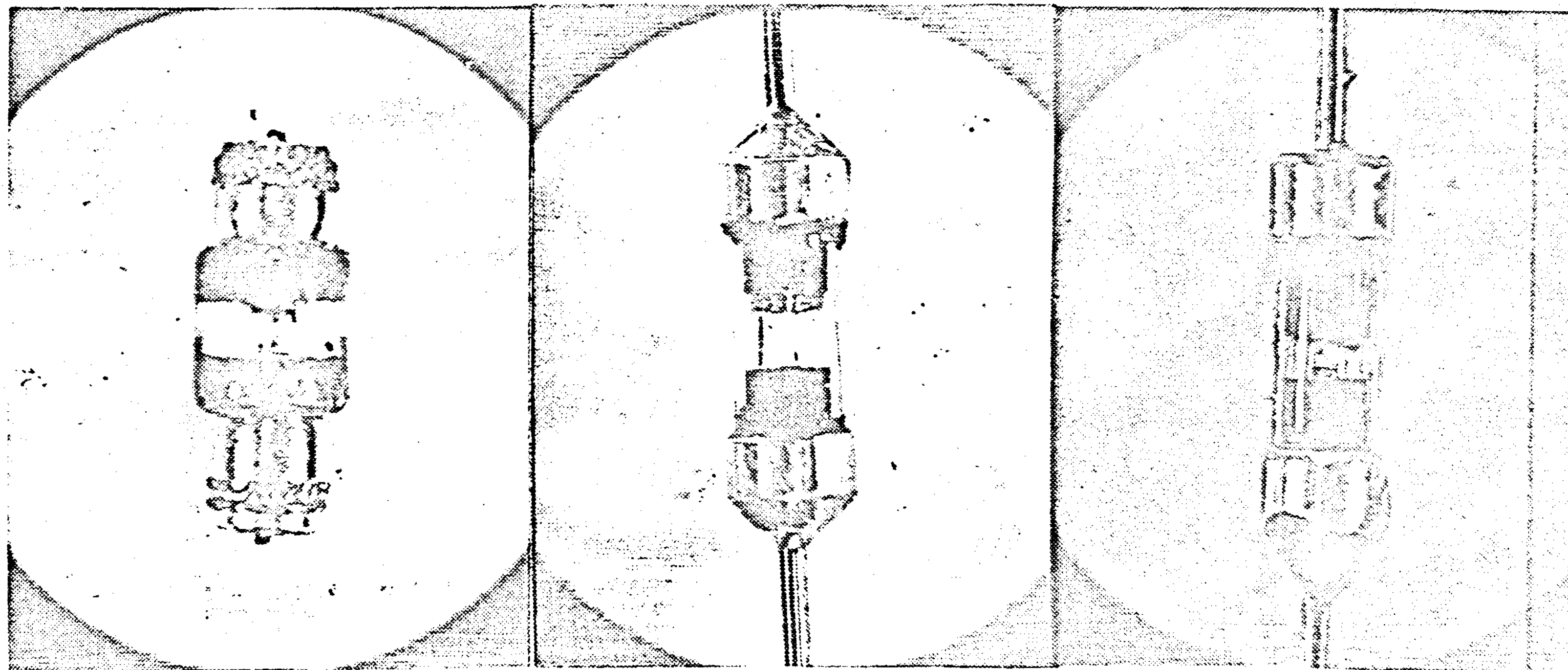

a. Point Contact b. Bonded c. Diffused

Figure 4. Cases used to encapsulate diodes used in this experiment.

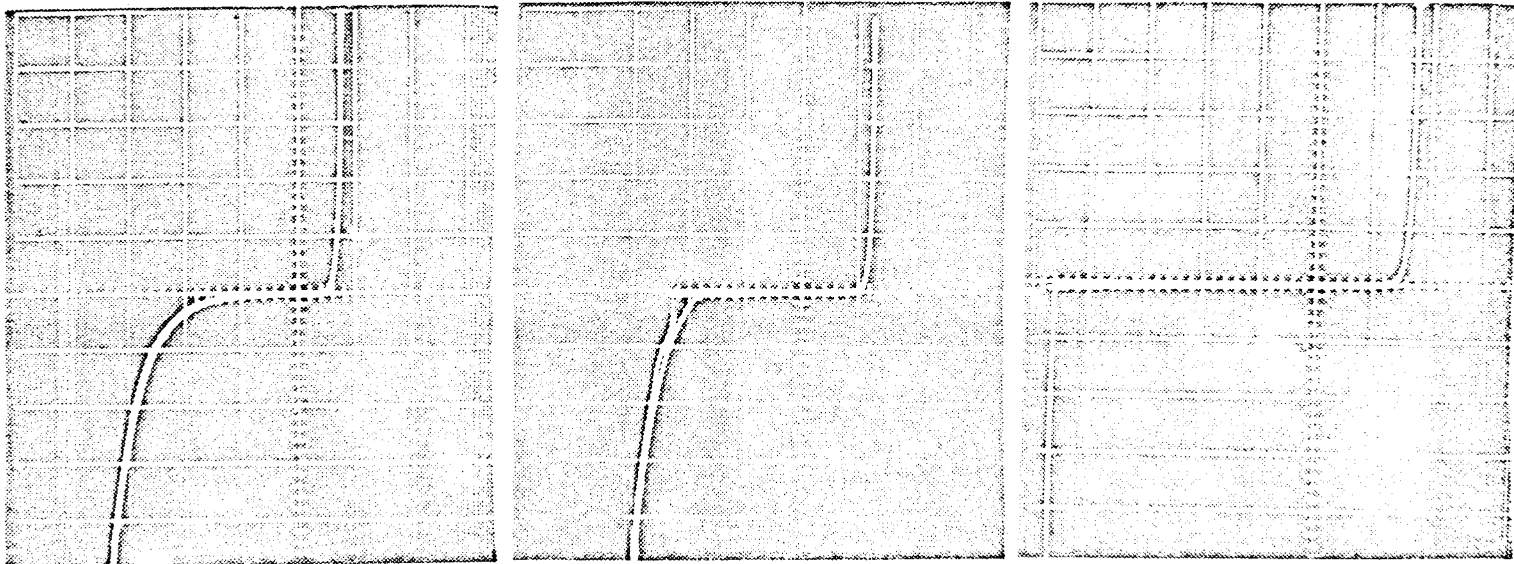

a. Point Contact　　　b. Bonded　　　c. Diffused

Forward: Horiz = 0.5 volts/major div
Vert = 20 μa/major div

Reverse: Horiz = 5 volts/major div
Vert = 20 μa/major div

Figure 5. Typical diode characteristics.

10 megohm input impedance but for the diffused diodes the reverse resistance is greater than 100 megohms and therefore most of the voltage falls across the diode. For the bonded and point-contact diodes, two measurements had to be made for high reverse-leakage diodes. One was taken as shown and one across the LC-meter. Placement of a voltmeter directly across the tested diodes caused transient variations due to pickup by the voltmeter chassis. Therefore, this method of voltage measurement was not used. This transient is effectively cancelled out by the 0.1 μf capacitor in the setup shown.

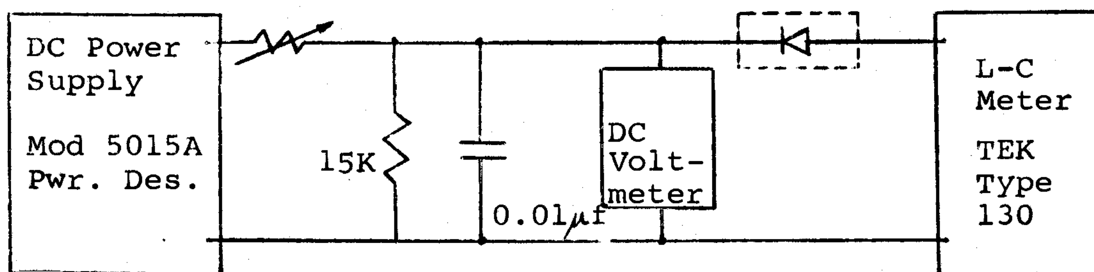

Figure 6. Schematic for Circuit Used to Measure Reverse-bias Capacitance as a Function of Reverse Voltage.

Figure 7 presents the schematic diagram for the multipurpose circuit that was used to measure the forward resistance, R_f, the reverse breakdown voltage, V_B, and the forward "knee" of the diode curve, V_f. It also served as the constant-current source for loading the diodes.

Both V_f and V_B were read directly off the diode

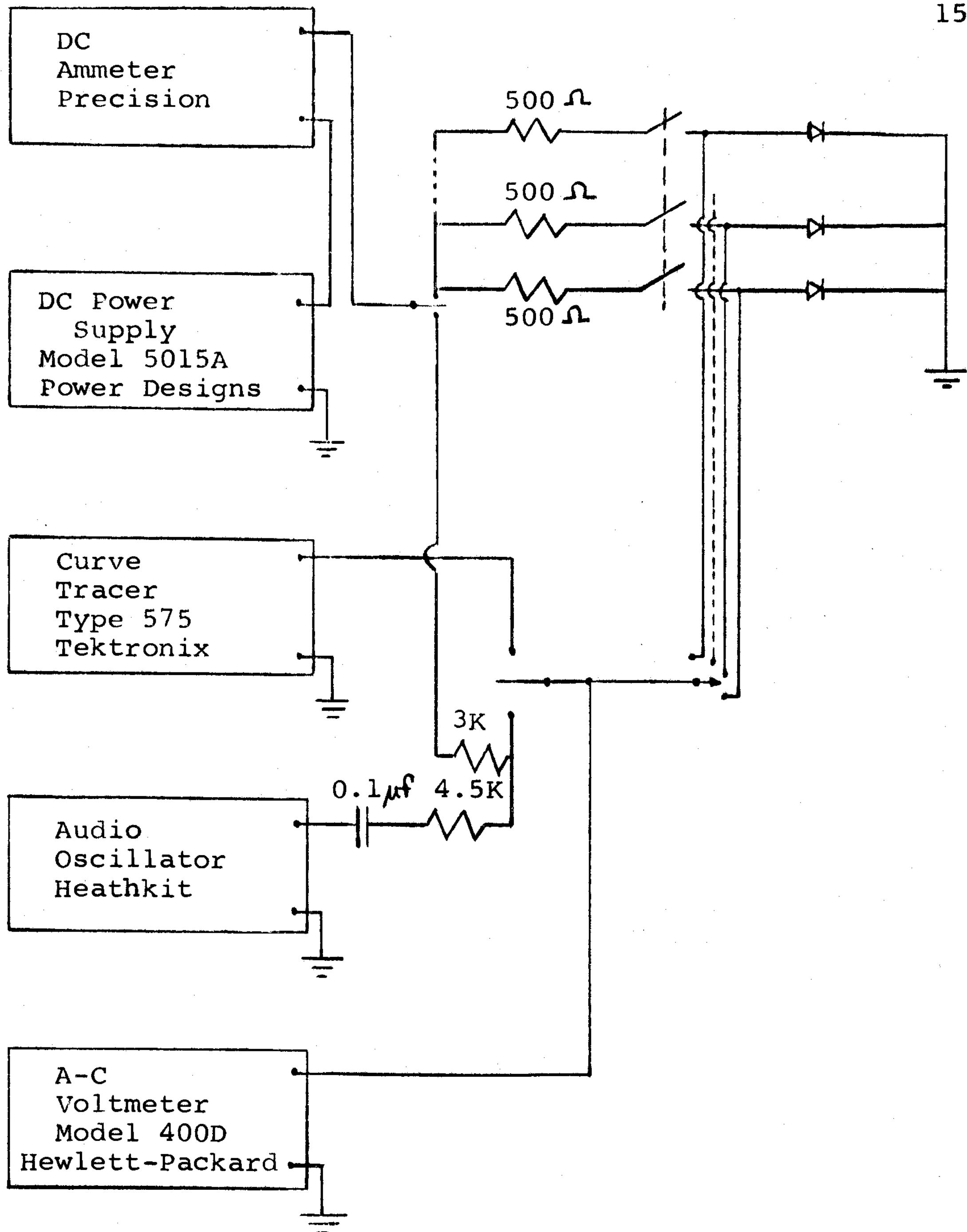

Figure 7. Schematic for Circuit Used as Constant-Current Power Supply and R_f, V_B and V_f Measuring Device.

curve tracer. V_f was the value of voltage at 100μa forward current. The voltage V_B was taken as that at which the reverse leakage current just exceeded 10μa.

The constant-current source consisted of ten parallel circuits. Table I shows the various errors in current in each branch under various loads.

The forward resistance, R_f, was measured at 10 ma. The voltmeter was calibrated by using known resistors as calibration points. Table II shows the errors at various resistances for each calibration point. The range of resistance values measured at each calibration point is also given in Table II. These tables are found in the appendix.

EXPERIMENTAL RESULTS

The experiment was carried out in three phases, each phase involving one of the three different diodes considered. Initial tests were conducted to determine the maximum current capabilities of the diodes, as overload failures were not of interest here. Due to variations in junction areas, however, this type of failure could not be completely eliminated.

It was found that ohmic dissipation in the diodes tended to heat them to such an extent that the measured parameters were affected, especially at the higher load currents. To overcome this a cooling period of fifteen minutes was allowed before taking any data. Figure 8 shows this transient variation in forward resistance for point-contact diodes loaded at 20 ma.

PHASE I. THE ZINC-DIFFUSED DIODES

Preliminary investigations showed that 70 ma was about the maximum load current that would yield a reasonable percentage of diodes which did not fail due to overloading. On this basis, load currents of 10 ma, 20 ma and 70 ma were chosen. Information on deterioration at 32 ma load current by Kan had been previously received. (11)

Figure 9 shows three examples of the type of curves

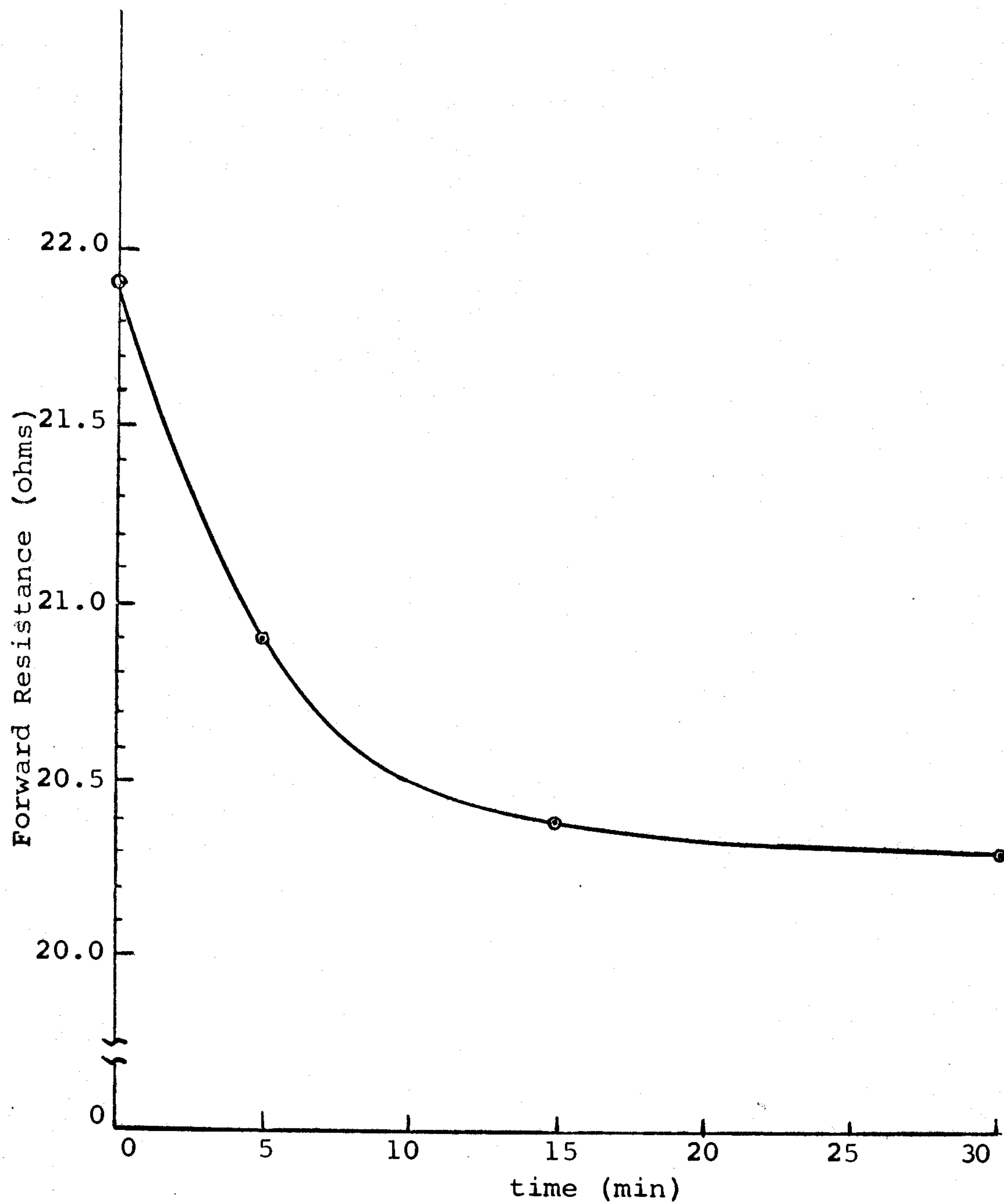

Figure 8. Transient Variation in Forward Resistance (at 10 ma) of Point-Contact Diodes with 20 ma Loading Due to Heating.

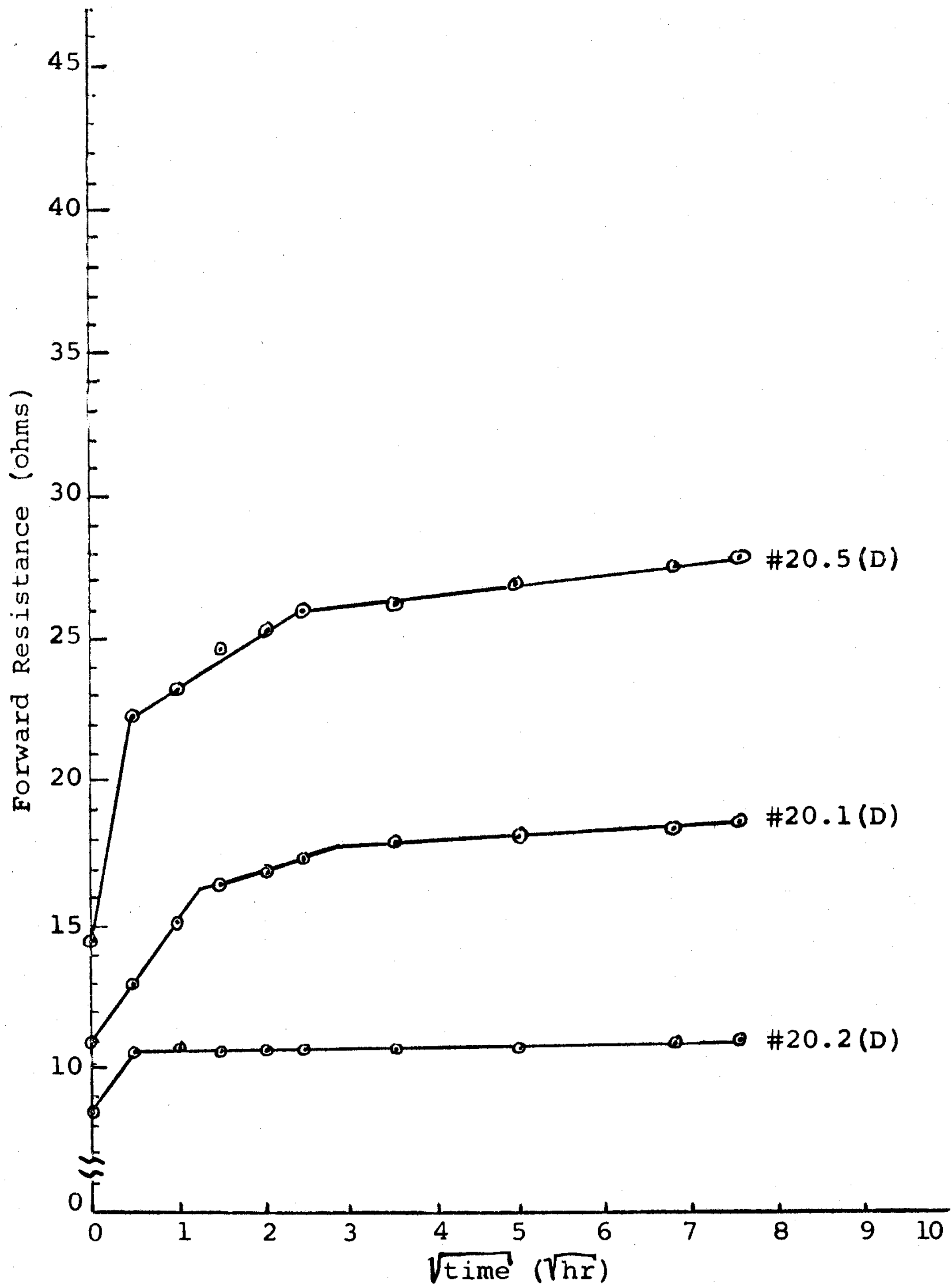

Figure 9. Typical Examples of Curves Plotted for Diffused Diodes at 20 ma Load Current.

that resulted from plotting the data taken at 20 ma load current. Even at this single load current very different values of changes were observed. It is reasonable to assume that part of this variation was due to differences in cross-sectional area. Also, since the initial change is so large some of these variations were not observed.

Assuming that the average cross-sectional area of any group of diodes equals that of any other group, the data becomes more understandable if plotted on a group average basis as shown in Figure 10. Here the curves for 10 ma, 20 ma, 32 ma and 70 ma are plotted.

For the 20 ma curve, three distinct slopes appear. This is similar to that observed by Shibata (19) in his experiments with zinc-diffused tunnel diodes.

Limitations of the LC-meter made accurate data on capacitance difficult to obtain. Simple arithmetic averaging was used to obtain the general direction in which changes took place. Figure 11 is a plot of the change in the constant n which exponentially relates reverse-bias capacitance to voltage, that is, $C \sim V^{-\frac{1}{n}}$. Each point represents the arithmetic average of a group of about ten diodes. To enhance the accuracy of the data, the reverse-bias capacitance was taken at -0.5 v, -1.0 v, -2.0 v, -5.0 v and -10.0 v. These were plotted and the slopes of the curves were graphically determined.

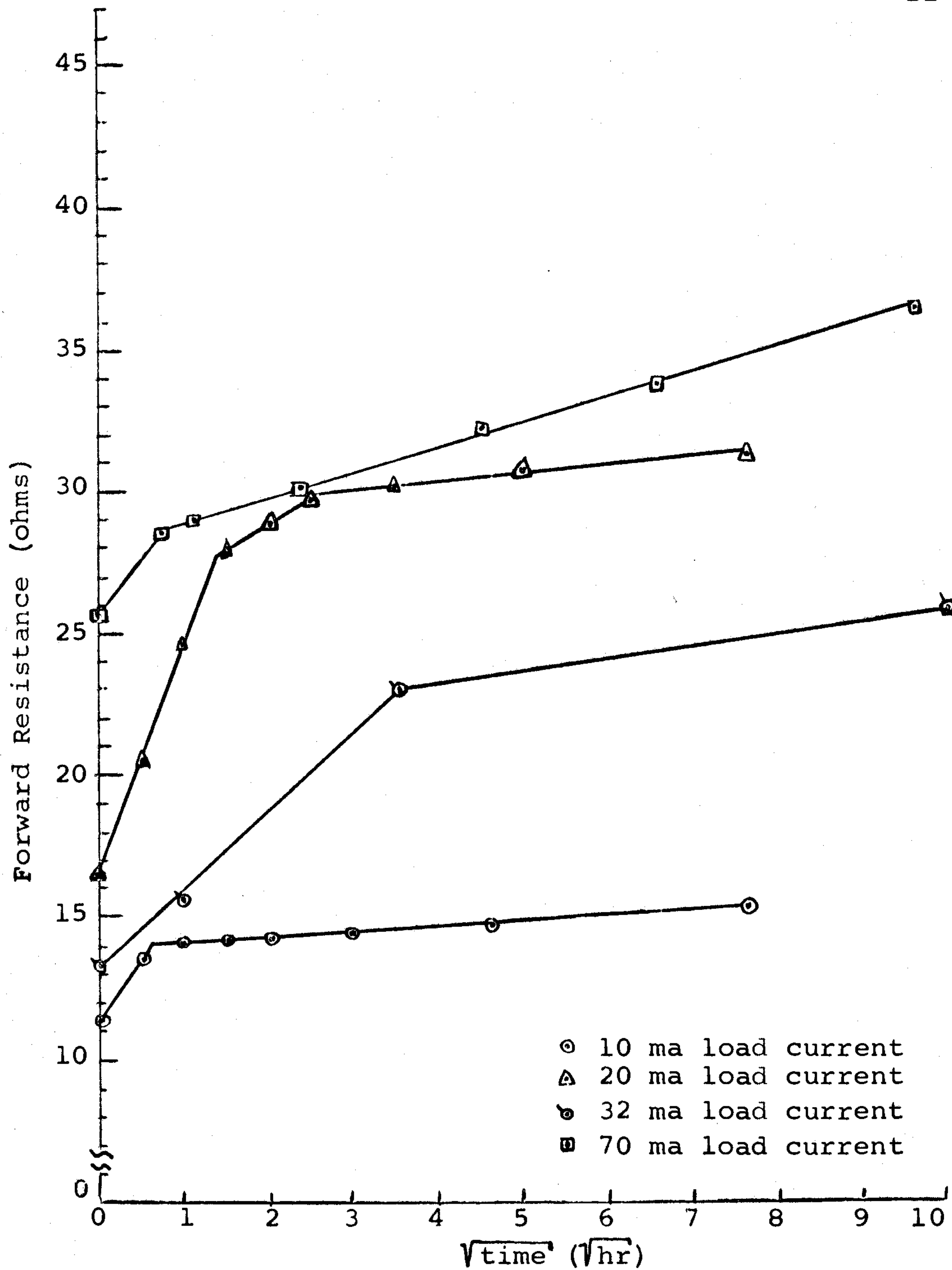

Figure 10. Average Change in Resistance for Zinc-Diffused Diodes at Different Load Currents.

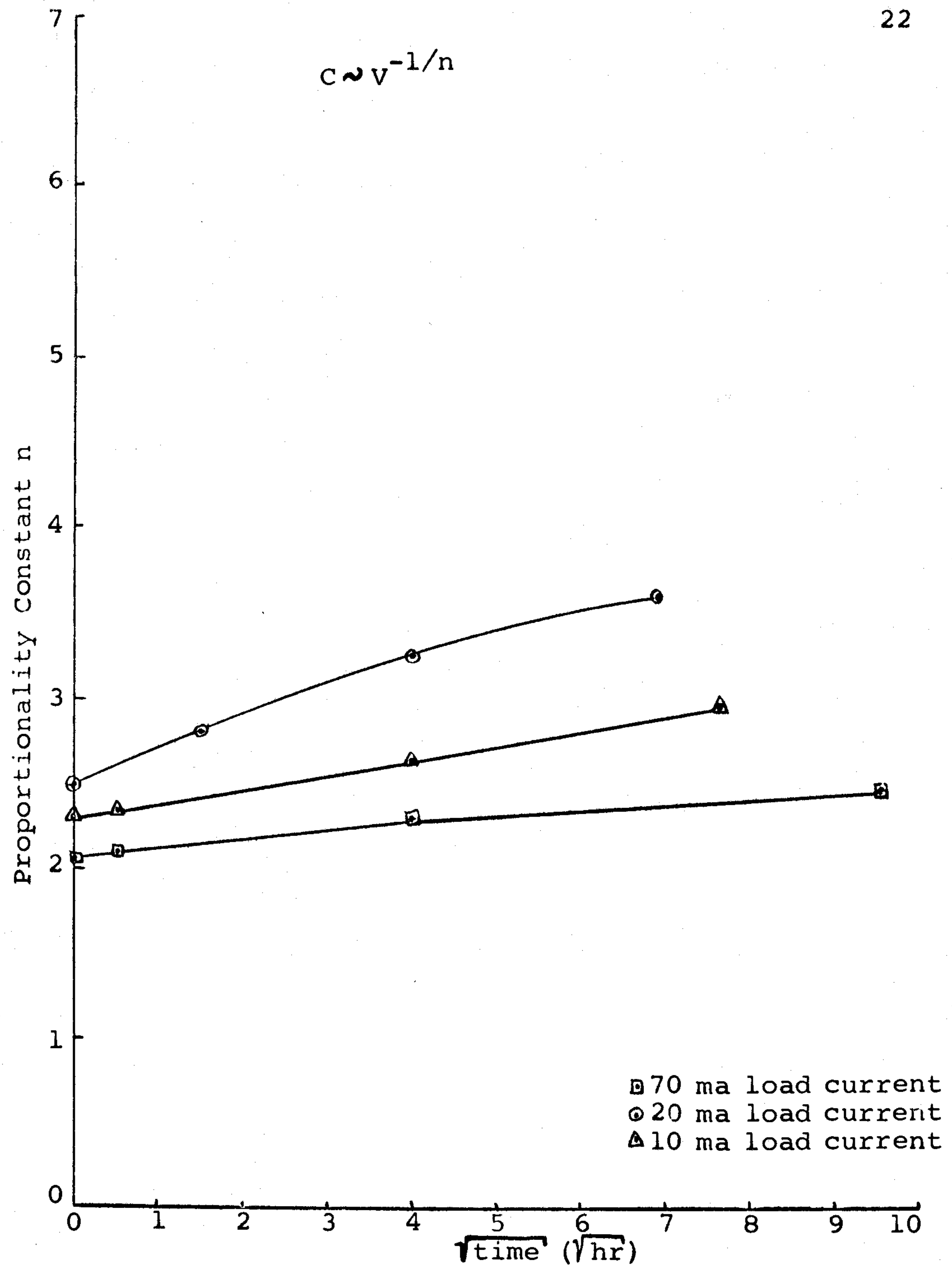

Figure 11. Change in Exponential Proportionality Constant n Relating Voltage to Reverse-Bias Capacitance.

The measured case capacitance for the diffused diodes varied between 0.08 to 0.09 picofarads. A value of 0.085 picofarads was used for case capacitance in all calculations.

The voltage at the forward knee of the diode curve in general tended to get smaller as the experiment progressed. Figure 12 shows the manner in which it varied with time. Very little observable change occurred after about two hours. The reverse breakdown voltage V_B changed very little during the experiment.

PHASE II. THE BONDED DIODES

Test load currents used for this phase of the experiment were 10 ma, 30 ma and 40 ma. Twenty diodes were used at each load current. The arithmetic average of resistance change is plotted in Figure 13. Figure 12 shows the change in the forward knee of the curve versus time.

For the 30 ma case the arithmetic-average change in V_f is nearly nonexistent. It is noted, however, that this is the result of the occurrence of diodes that increased the value of V_f as well as those that decreased with time.

In averaging the resistance changes, data points at which diodes exhibited an unstable value were excluded. This was done for two reasons. First, the resulting

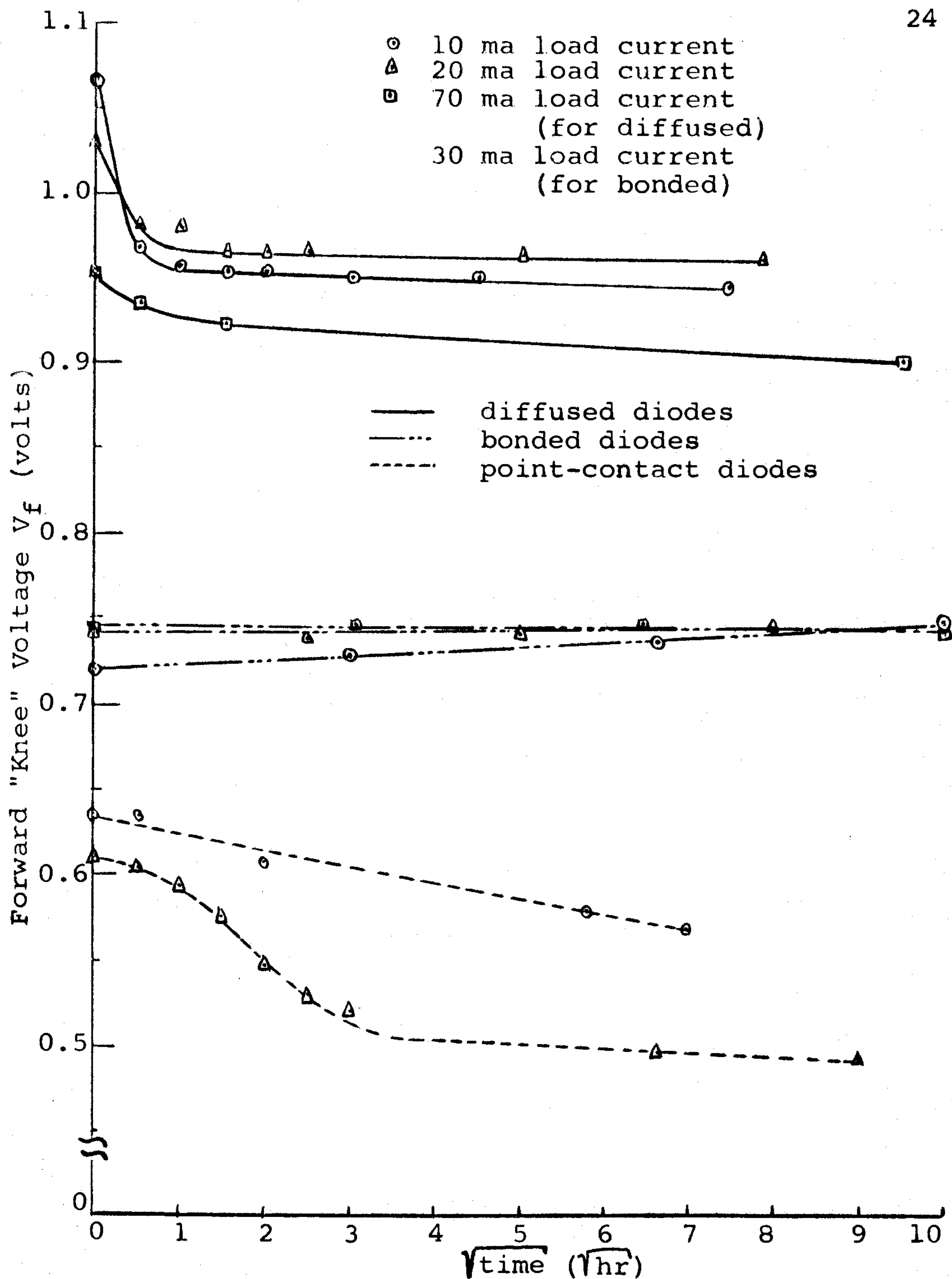

Figure 12. Changes in V_f for the Three Different Diode Types.

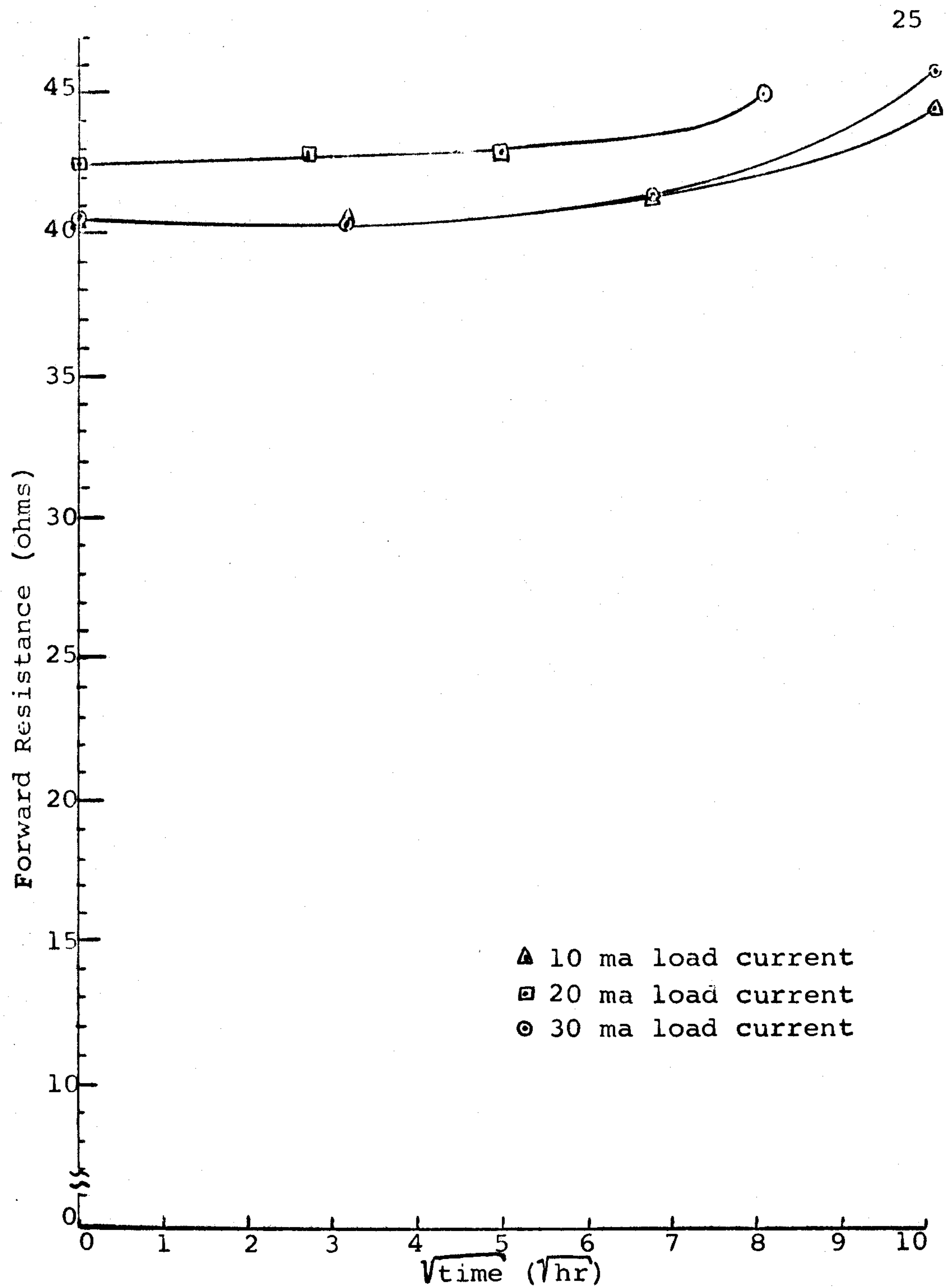

Figure 13. Forward Resistance Change for Bonded GaAs Diodes.

data would have been distorted since these values usually indicated changes in resistance of the order of a hundred ohms. Secondly, it was impossible to assign an accurate value to the resistance because of the instability.

PHASE III. THE POINT-CONTACT DIODES

The load currents selected for this phase of the experiment were 10 ma and 20 ma. The occurrence of a great number of diodes exhibiting abrupt changes in characteristics made data obtained for 30 ma and 40 ma load currents difficult to interpret. An example of this type of behavior is shown in Figure 14. Because of the size of the metal whisker, burn-out failures (1) were not observed. Instead the metal-semiconductor rectifying junctions tended to become ohmic. Changes in forward resistance for the two load currents are shown in Figure 15. Variations of V_f are found in Figure 12.

The reverse breakdown voltage for the diffused diodes changed very little during the experiment. However, for the point-contact diodes this parameter changed measurably. Figure 16 shows this change.

Reverse-bias capacitance measurements were difficult to obtain since the reverse leakage increased so rapidly. On the average it appears that the diodes possessed a large enough reverse breakdown voltage to yield capacitive change measurements, but on an individual basis

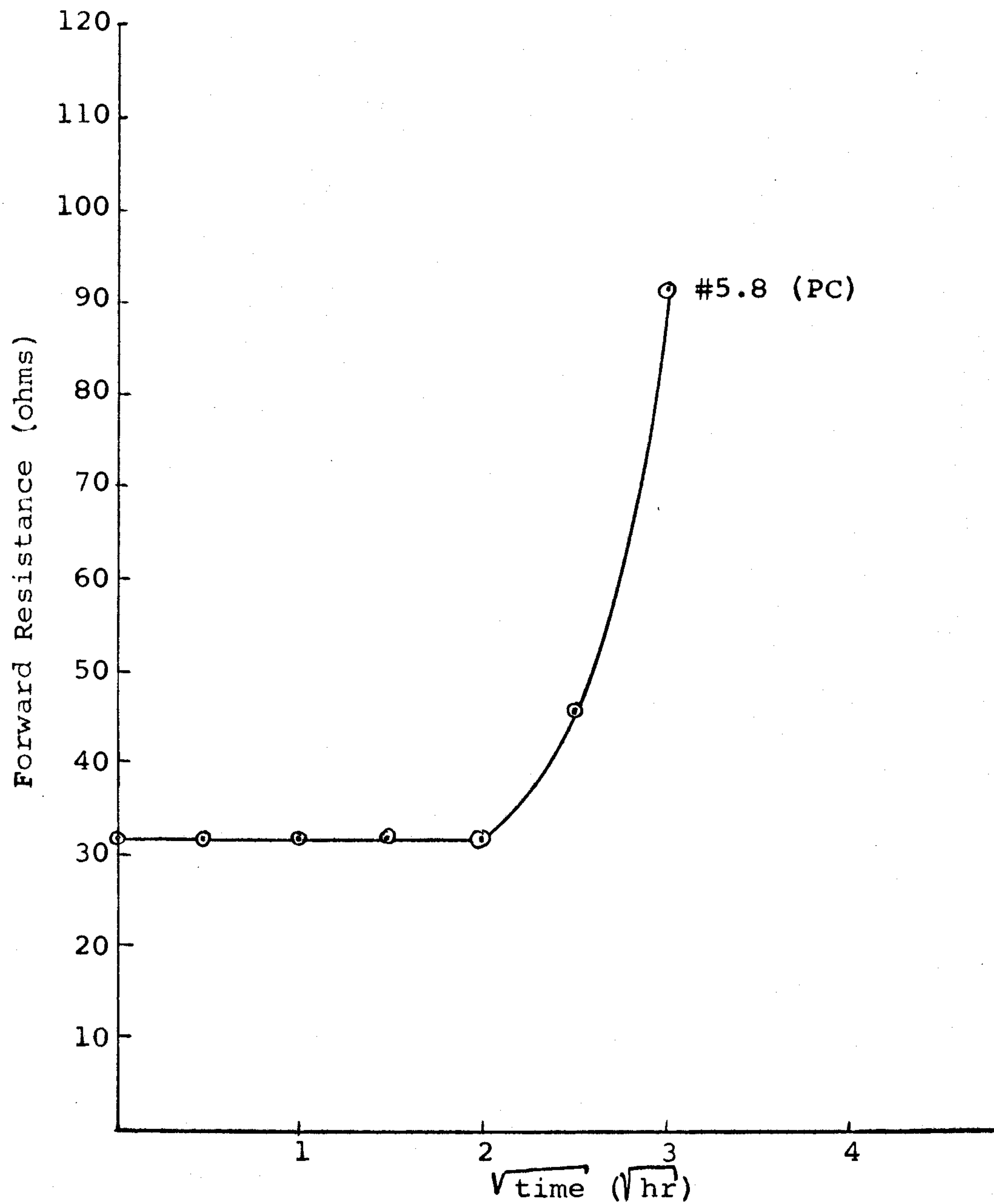

Figure 14. Example of a Point-Contact Diode Exhibiting Abrupt Change in Forward Resistance.

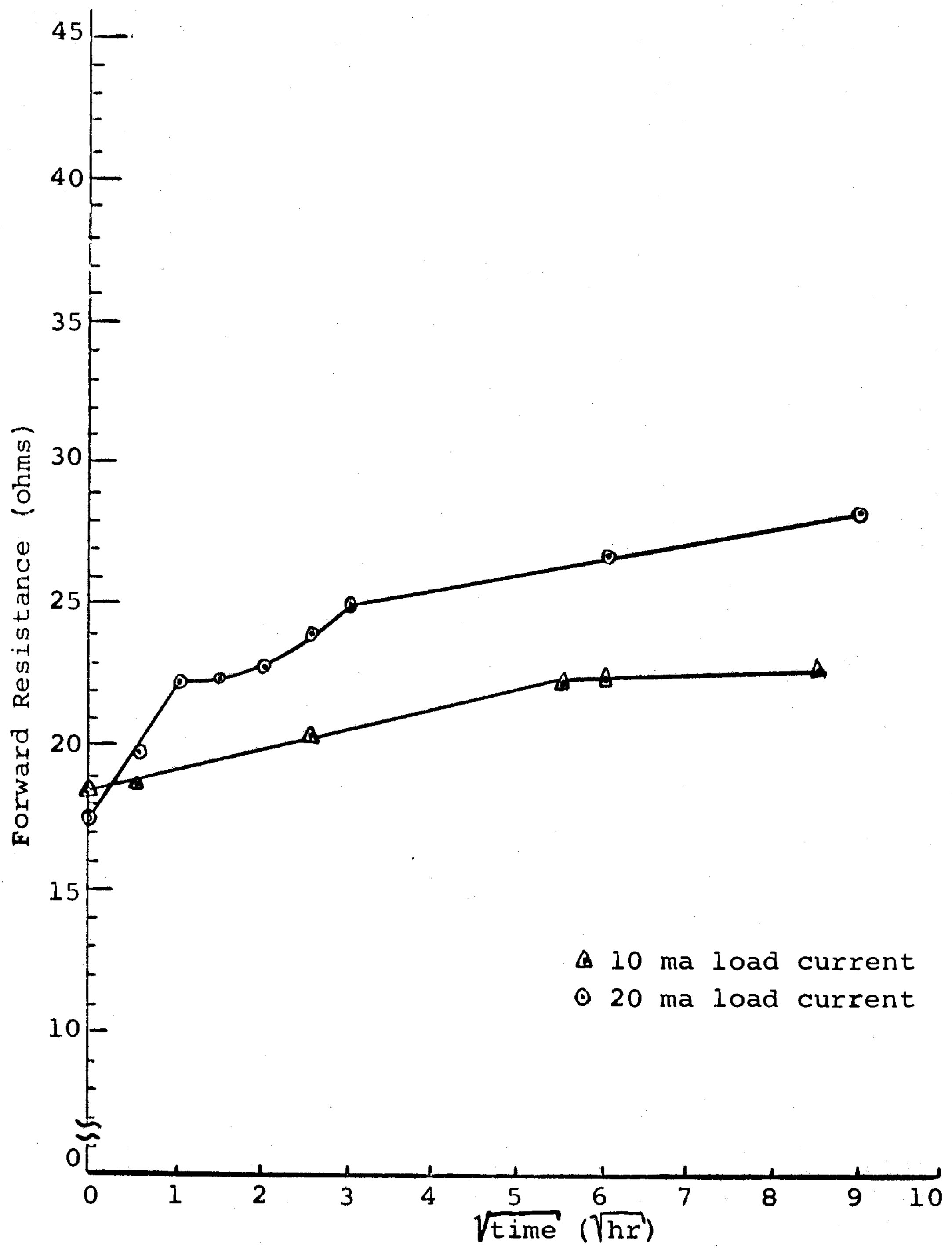

Figure 15. Changes in Resistivity of Point-Contact Diodes.

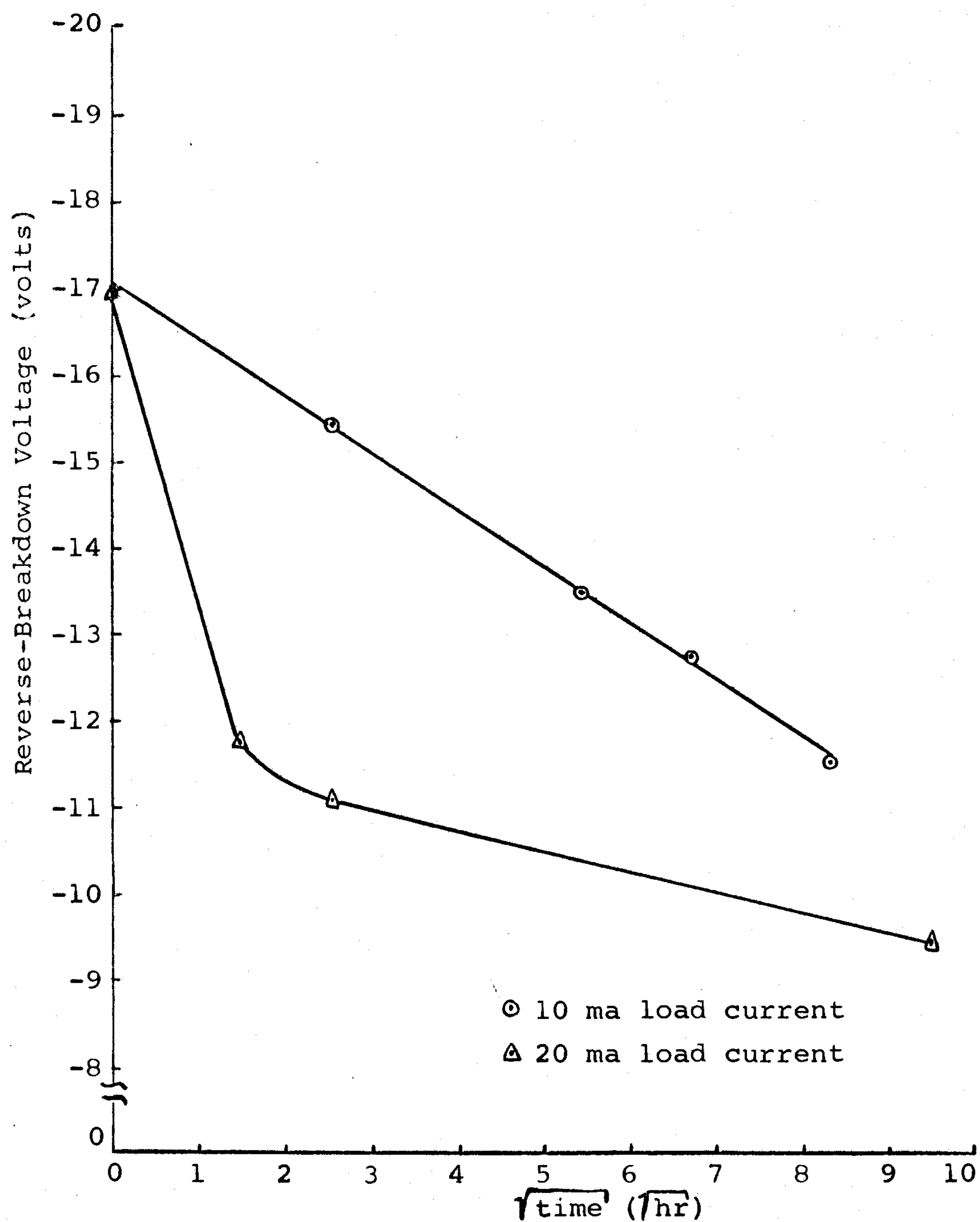

Figure 16. Change in V_B for Point-Contact Diodes.

the reverse breakdown of a large number was less than -4 volts, making useful measurement of this kind impossible.

CORRELATION OF THE RESULTS

Figures 17, 18 and 19 show the changes in characteristics for the three different types of diodes at 20 ma load current. This serves to unify the three phases of the experiment.

Changes in the bonded diodes are very small compared to the diffused and the point-contact types. The point-contact diodes exhibit the greatest change in forward resistance of 20 ma load current. As pointed out above the forward "knee" of the bonded diodes increases with time while it decreases for the point-contact and the diffused diodes.

The exponential proportionality constant n is not shown in a composite figure since this information could not be obtained for the point-contact case.

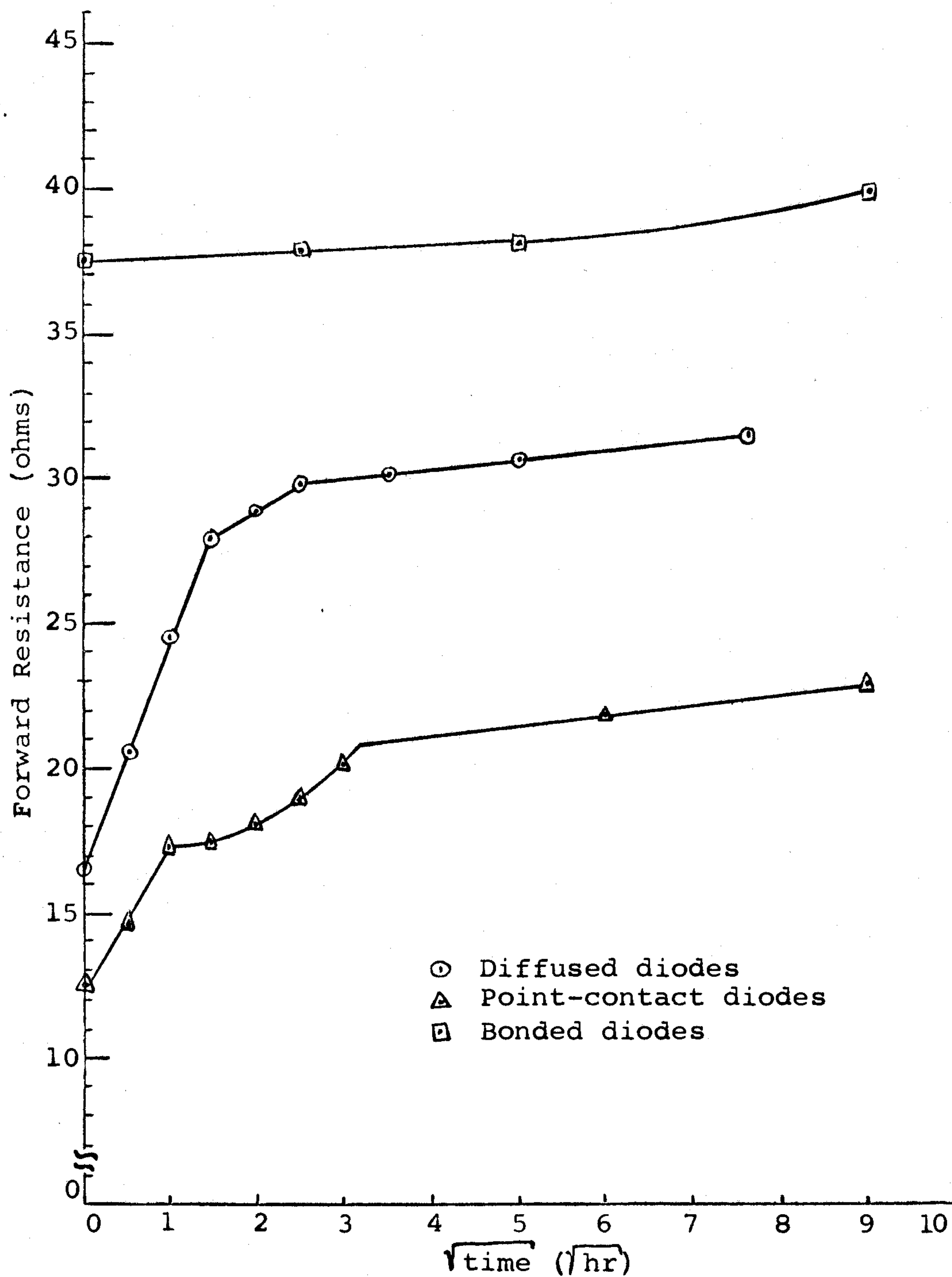

Figure 17. Comparison of Changes in R_f of the Different Diode Types at 20 ma.

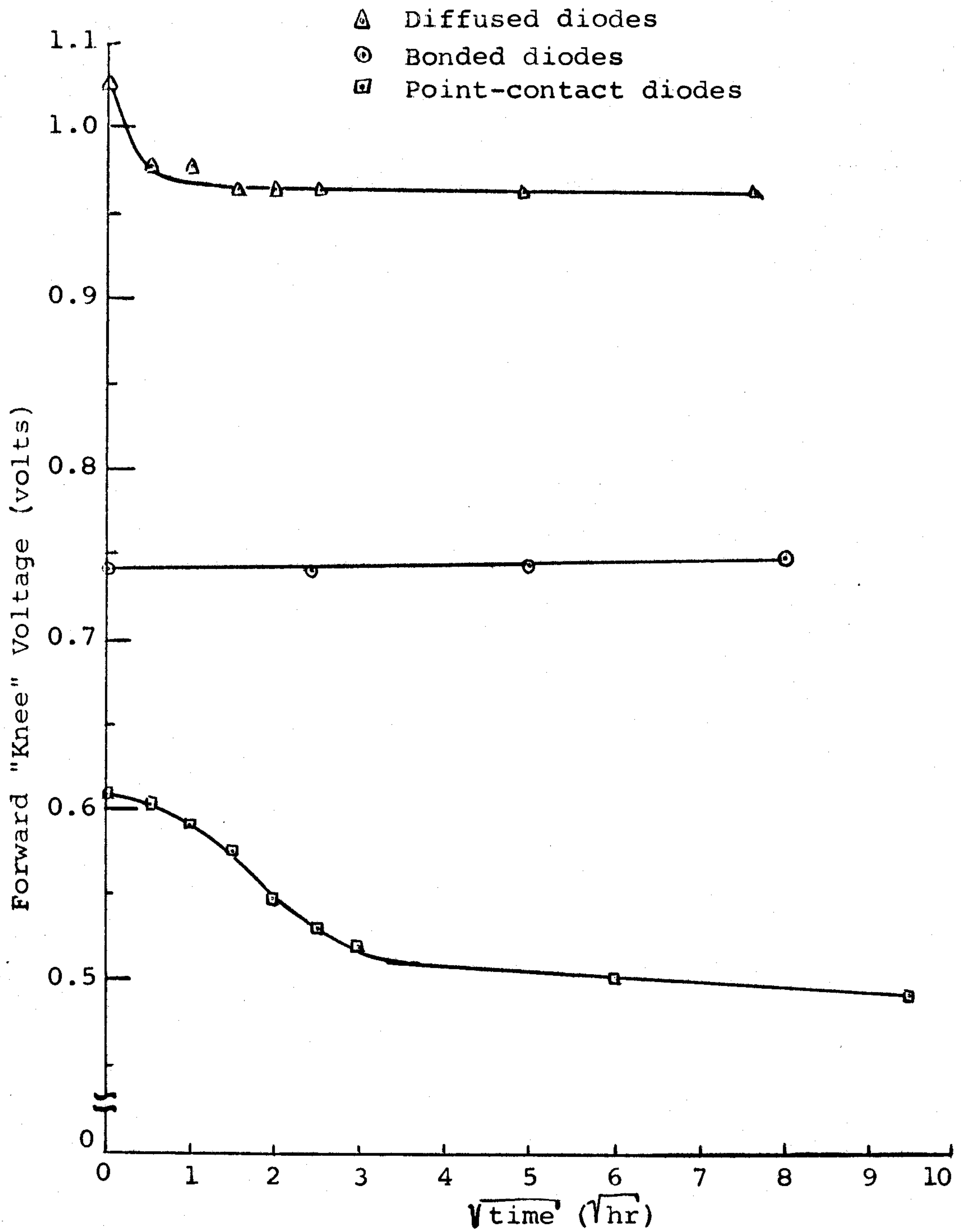

Figure 18. Comparison of Changes in V_f of the Different Diode Types at 20 ma.

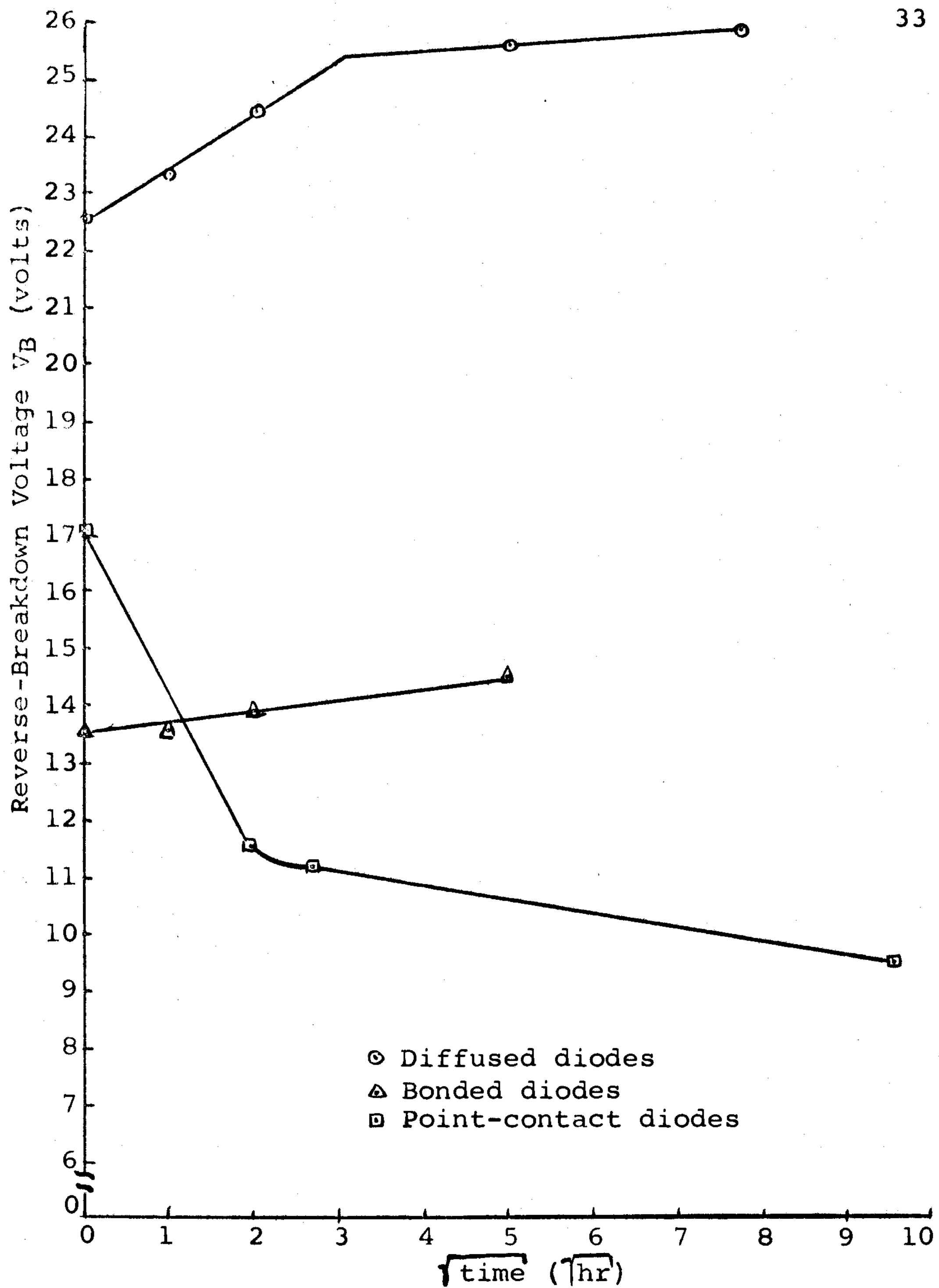

Figure 19. Comparison of Changes in V_B of the Different Diode Types at 20 ma.

DISCUSSION OF THE RESULTS

Three types of GaAs diodes, the zinc-diffused, the bonded and the point-contact, were studied in this experiment. Of the three, the bonded diodes showed the least change in characteristics. The forward resistance varied approximately as the linear relation $R = 0.5t^{\frac{1}{2}}$. V_f tended to increase in a similar manner contrary to the results of the two other diode types.

An increase in the barrier height at the metal-semiconductor junction explains these results very nicely. V_f is increased since more energy is required before an appreciable number of carriers can be accelerated over the barrier. The diode equation gives the relation $I = I_s \exp (qV/kT)$ for forward-bias conditions. V is the junction voltage and equals the applied voltage minus the bulk resistance drop and the barrier potential. An increase in the barrier potential tends to flatten the V-I plot. Thus for any given current the slope of the curve increases as the barrier potential increases, hence, increasing R_f.

In the point-contact diodes, R_f tended to increase while V_f decreased. This is contrary to the bonded diodes although both are metal-semiconductor junctions. It has been noted in the experimental data that when subjected to high current the metal-semiconductor rectifying

junctions of the point-contact diodes became ohmic. Point-contact diodes are known to be highly dependent on surface conditions. (3) An increase in surface recombination states results in a linear forward characteristic since the injected carriers recombine with very short lifetimes and do not cause an exponential increase in forward current as predicted by the diode equation. The reverse breakdown voltage also decreased, becoming more ohmic in nature.

The curves in Figure 15 show that the forward resistance increases as load current is applied starting from a resistive value greater than 10 ohms. For diodes subjected to very high currents the final resistance approached 10 ohms. This would require a maximum in the curve and indicate possibly two different mechanisms of deterioration. However, high currents had to be used to attain the near-ohmic deteriorated diodes. This could have created high enough temperature to cause alloying in such a manner that the metal-semiconductor barrier was removed. Such temperatures may not be possible to obtain at the lower currents of the experiment and, hence, the curves could increase indefinitely as shown.

The results obtained for the diffused diodes yielded the best data from the standpoint of analysis. Figure 9 shows the changes in resistance at various load

currents. For the 20 ma case there are three distinct slopes. This is similar to the observations made by Shibata (19) on the deterioration of tunnel diodes.

Longini (14) has made a study of rapid zinc diffusion in gallium arsenide and has arrived at the formula $F(V) = F(0) \exp (eV/kT)$ for the impurity flux $F(V)$ across a junction biased by V. $F(0)$ is the impurity flux with no bias applied. Combining this equation with the well known diffusion equation $D = D_o \exp (-E/kT)$, $F(V) = D_o \exp (-E/kT) \exp (eV/kt)$. For gallium arsenide E is about 2.49 ev and D_o is about 15.

The initial slope of the 20 ma curve in Figure 9 gives $R_1/R_o = 1.69$ where R_1 is the resistance at T=1 hour and R_o is the resistance at t=0. Black (1) found the relation between resistivity and free carrier density for gallium arsenide and using a resistivity of 0.02Ω-cm, a change of 1.69 in resistivity is associated with a change in carrier density of 3.9×10^{20} carriers/hour or 1.08×10^{18} carriers/sec. This yields $1.08 \times 10^{18} = 15 \exp (-2.49/kT) \exp (1.2/kt)$. Solving for the junction temperature T, T = 107° C which is a reasonable value. Without making use of Longini's idea, the junction temperature is calculated to be 487° C, a highly improbable value.

As Rediker (17) indicated, it is difficult to

determine junction area since the current density throughout the cross-section is not uniform. However, considering the averaged characteristics in Figure 9 and determining the final slopes of each curve, a plot of $\Delta R/\Delta\sqrt{t}$ versus I yields a linear plot as shown in Figure 20. The constant slope has the value 22 ohms/hour$^{1/2}$- amp showing that the deterioration is a function of both the square root of time and the magnitude of load current.

For the change in reverse-bias capacitance a built-in potential of 1.2 volts was assumed as determined by Lowen. (16) The results show that for the 10 ma case the capacitance varies at first as $V^{-1/2.4}$ and gradually changes until it varies as $V^{-1/2.9}$. In the 20 ma case the voltage dependence varied from $V^{-1/2.3}$ to $V^{-1/3.7}$. These indicate the type of junction varies from a near step junction to a graded one as would result if zinc or some other electrically active element diffused under the application of an electric field.

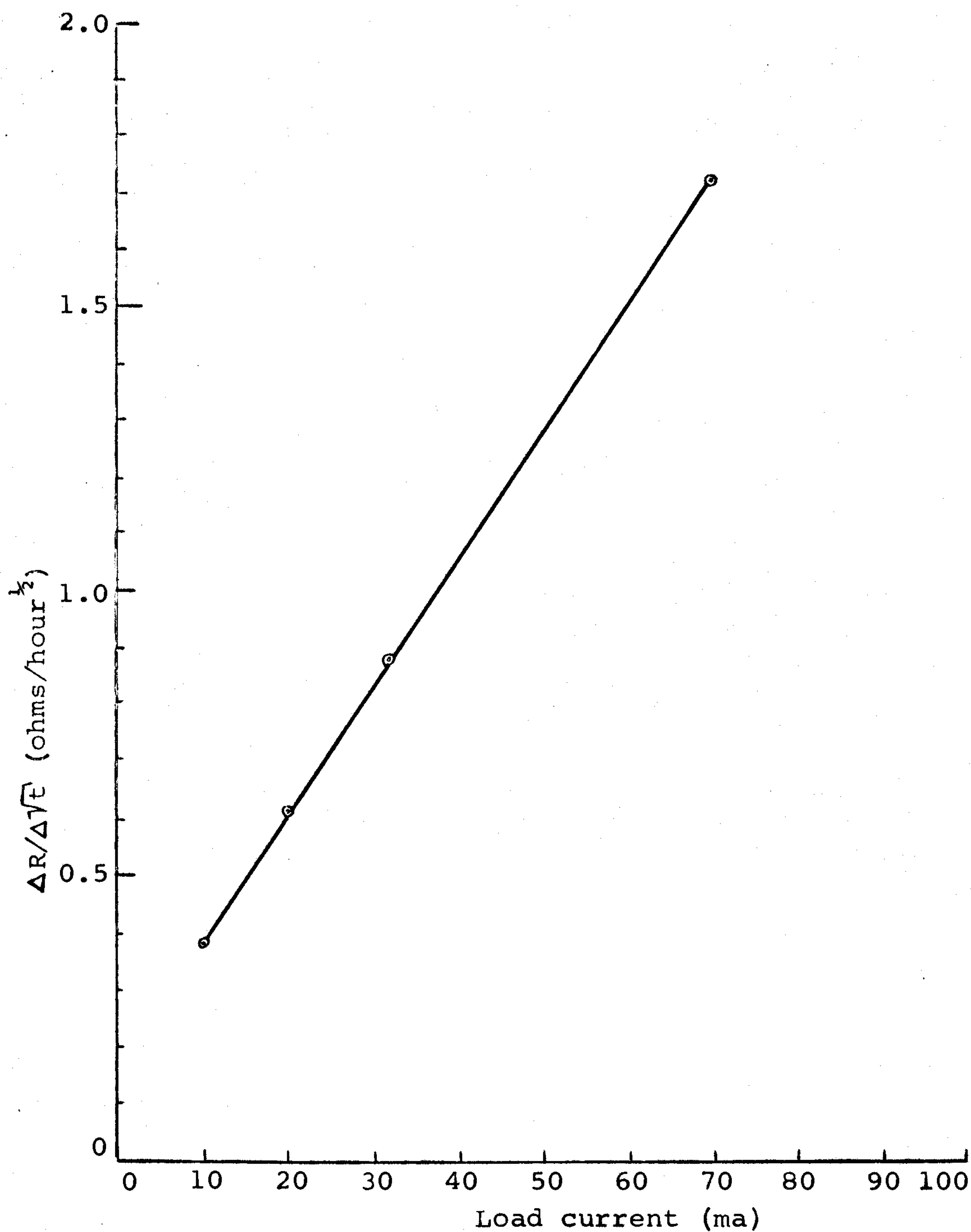

Figure 20. A Plot of $\Delta R/\Delta\sqrt{t}$ as a Function of Load Current for Zinc-Diffused Diodes.

SUMMARY

In this experiment three different types of GaAs diodes were studied. These were point-contact, bonded, and zinc-diffused diodes. Various load currents were applied and the change in characteristics were observed.

All three types of diodes tested experienced increases in forward resistance with the application of load current. In the zinc-diffused diodes a large initial change was noticed and this might be attributed to rapid zinc diffusion as suggested by Longini. (14) The final slope corresponds to the final slopes of the two other types of diodes as the rate of deterioration is similar. The mechanism causing the deterioration may be the same and doesn't appear to be due to zinc migration.

The absolute value of load current is related to the change in resistance as 22 ohms/hour$^{\frac{1}{2}}$ - amp. Difficulty in determining actual junction cross-sectional area prevented relating the changes to current density. However, the change in resistance is seen to be directly proportional to both the square root of time and to the load current.

In the extreme case, the exponential relation between the capacitance and reverse-bias voltage varied for the diffused diodes between $V^{-1/2.3}$ to $V^{-1/3.7}$. This indicates a change from a step junction to a PIN

type junction. The voltage at the forward "knee" of the diode curve decreased for the diffused and point-contact diodes but increased for the bonded diodes. An increase in junction barrier height may be responsible for the variation in the bonded diodes while an increase in surface recombination states may be responsible for the decrease in the point-contact case. The spreading of the pn junction by diffusion of an electrically active element is a possible cause of the change in the diffused diodes.

BIBLIOGRAPHY

1. Black, J. Correlation of electrical measurements with chemical analysis in zinc- and cadmium-diffused GaAs. Journal of the Electrochemical Society 111:924-928. 1964.

2. Blanc, Joseph, Richard H. Bube and Leonard R. Weisberg. Behavior of lattice defects in GaAs. Journal of Physics and Chemistry of Solids 25:225-241. 1964.

3. Bridges, H. E., J. H. Scaff and J. N. Shife (eds.). Transistor technology. Vol. I. New York, Van Nostrand, 1958. 661 p.

4. Chang, L. L. and G. L. Pearson. The solubilities and distribution coefficients of zinc in GaAs and GaP. Journal of Physics and Chemistry of Solids 25:23-30. 1964.

5. Goldstein, B. Diffusion in compound semiconductors. Physical Revier 121:1305-1311. 1961.

6. ____________. Diffusion of cadmium and zinc in gallium arsenide. Physical Review 118:1024-1027. 1960.

7. Hall, R. N. and J. H. Racette. Behavior of Cu in Ge, Si and GaAs. Bulletin of the American Physical Society 7:234. 1962.

8. Hunter, Lloyd P. (ed.) Handbook of semiconductor electronics. New York, McGraw-Hill, 1962. 1 vol.

9. Jenney, D. A. A gallium arsenide microwave diode. Proceedings of the Institute of Radio Engineers 46:717-722. 1958.

10. Jost, W. Diffusion in solids, liquids and gases. New York, Academic Press, 1952. 558 p.

11. Kan, Arnold. Semiconductor Research Department. Tektronix Co. Private communication. Beaverton, Oregon. 1965.

12. Larrabee, Graydon B. The contamination of semiconductor surfaces. Journal of the Electrochemical Society 108:1130-1134. 1961.

13. Logan, R. A., A. G. Chynoweth and B. G. Cohen. Avalanche breakdown in gallium arsenide p-n junctions. Physical Review 128:2518-2523. 1962.

14. Longini, R. L. Rapid zinc diffusion in gallium arsenide. Solid State Electronics 5:127-130. 1962.

15. Looney, James C., Ass't. Professor, Department of Electrical Engineering, Oregon State University. Private communication. Corvallis, Oregon. 1965.

16. Lowen, J. and R. H. Rediker. Gallium arsenide diffused diodes. Journal of the Electrochemical Society 107:26-29. 1960.

17. Rediker, R. H. and T. M. Quist. Properties of GaAs alloy diodes. Solid State Electronics 6:657-665. 1963.

18. Sharpless, W. M. High-frequency gallium arsenide point-contact rectifiers. Bell System Technical Journal 38:259-269. 1959.

19. Shibata, A. Rapid impurity diffusion in GaAs Esaki diodes. Solid State Electronics 7:215-218. 1964.

20. Valdes, Leopoldo B. The physical theory of transistors. New York, McGraw-Hill, 1961. 370 p.

21. Weiser, K. Ratio of interstitial to substitutional zinc in GaAs and its relation in zinc diffusion. Journal of Applied Physics 44:3387-3389. 1963.

APPENDIX

TABLE I. Branch Currents Under Different Load Conditions with 100 ma Total Load Current.

Br. No.	Branch Current (with all other branches short-circuited)			
	0Ω load	20Ω load	40Ω load	60Ω load
1	10.1	9.7	9.3	9.1
2	10.0	9.6	9.3	9.0
3	10.1	9.7	9.4	9.1
4	9.9	9.6	9.2	9.0
5	10.0	9.6	9.3	9.1
6	10.0	9.6	9.3	9.0
7	9.9	9.5	9.3	9.0
8	10.0	9.6	9.2	9.1
9	10.0	9.6	9.3	9.1
10	9.9	9.6	9.2	9.0

TABLE II. Calibration Errors at Various Calibration Points.

Calib. Resistance \ Actual Load	10Ω	20Ω	30Ω	40Ω	60Ω	90Ω	Range Used
10Ω	10.0	20.0	29.5	39.0	58.5	85.0	0-15Ω
20Ω	10.0	20.0	29.0	39.5	59.5	87.0	15-25Ω
30Ω	10.2	20.1	30.0	40.0	59.5	87.0	25-35Ω
40Ω	10.2	20.2	30.0	40.0	60.5	88.0	35-50Ω
60Ω	10.2	20.1	30.5	40.0	60.0	87.5	50-75Ω
90Ω	10.7	20.9	31.5	40.5	60.7	90.0	75-105Ω